Nuclear Engineering and Technology 48 (2016) 448–456

Available online at ScienceDirect

Nuclear Engineering and Technology

journal homepage: www.elsevier.com/locate/net

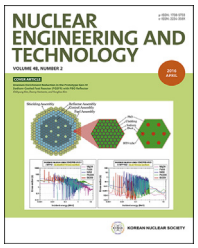

Original Article

Assessment of Mass Fraction and Melting Temperature for the Application of Limestone Concrete and Siliceous Concrete to Nuclear Reactor Basemat Considering Molten Core–Concrete Interaction

Hojae Lee [a,*], *Jae-Leon Cho* [b], *Eui-Sik Yoon* [c], *Myungsug Cho* [d], *and Do-Gyeum Kim* [a]

[a] *Korea Institute of Civil Engineering & Building Technology, 283 Goyangdae-ro, Ilsanseo-gu, Goyang-si, Gyeonggi-do 10223, Republic of Korea*

[b] *Korea Hydro & Nuclear Power Co., Shinam-ri, Seosaeng-myeon, Ulju-gun in Ulsan Metropolitan City 45014, Republic of Korea*

[c] *Korea Institute of Nuclear Safety, 62 Gwahak-ro, Yuseong-gu, Daejeon 34142, Republic of Korea*

[d] *Korea Hydro & Nuclear Power Co., Central Research Institute, 70, Yuseong-daero 1312beon-gil, Yuseong-gu, Daejeon 34101, Republic of Korea*

ARTICLE INFO

Article history:
Received 6 March 2015
Received in revised form
23 December 2015
Accepted 30 December 2015
Available online 2 February 2016

Keywords:
Concrete
Mass Fraction
Melting Temperature
Molten Core–Concrete Interaction
Thermogravimetric Analysis

ABSTRACT

Severe accident scenarios in nuclear reactors, such as nuclear meltdown, reveal that an extremely hot molten core may fall into the nuclear reactor cavity and seriously affect the safety of the nuclear containment vessel due to the chain reaction caused by the reaction between the molten core and concrete. This paper reports on research focused on the type and amount of vapor produced during the reaction between a high-temperature molten core and concrete, as well as on the erosion rate of concrete and the heat transfer characteristics at its vicinity. This study identifies the mass fraction and melting temperature as the most influential properties of concrete necessary for a safety analysis conducted in relation to the thermal interaction between the molten core and the basemat concrete. The types of concrete that are actually used in nuclear reactor cavities were investigated. The H_2O content in concrete required for the computation of the relative amount of gases generated by the chemical reaction of the vapor, the quantity of CO_2 necessary for computing the cooling speed of the molten core, and the melting temperature of concrete are evaluated experimentally for the molten core–concrete interaction analysis.

* *Corresponding author.*
E-mail address: h.lee@kict.re.kr (H. Lee).

http://dx.doi.org/10.1016/j.net.2015.12.014

1. Introduction

In case of damage to the nuclear reactor vessel in a severe accident, a reaction may occur between the high-temperature molten core and the concrete of the cavity basemat at the base of the containment vessel. Such reactions will lead to erosion and produce inflammable gas (H_2), inert gases, and fission products, which will result in an increase of the pressure inside the containment vessel, affecting its safety. Among the major factors that influence the reaction between the molten core and concrete, the types and relative amounts of gases generated by the chemical reaction between the molten substances, concrete, and vapor, together with the melting speed of the cavity basemat, are very important when determining the thickness and area of the cavity basemat and for designing the containment vessel.

In the 1990s, the Argonne National Laboratory in Lemont, IL, USA carried out experimental and analytical research on molten core–concrete interaction (MCCI) by pouring water on the top of the molten core, using MACE test equipment [1]. The MACE experiment led to the presumption of the existence of cooling mechanisms for molten material, such as bulk cooling, water ingression, melt eruption, and crust failure. This presumption stressed the necessity of gathering additional experimental data to provide a more reliable basis for understanding each of these cooling mechanisms, solving the cooling problem of the molten core welling out of the reactor by means of experimental models, and settling the uncertainty problems related to MCCI.

However, despite the need for experimental data to provide a reliable basis, most of the research related to MCCI to date has been performed in the fields of nuclear power and mechanics, where concrete is assumed simply as a unique object the properties of which are applied in a model for the analysis. Moreover, the past experimental approaches for MCCI focused primarily on the molten matters with regard to the phenomena provoked by the contact between concrete and the molten core, such as melt eruption, water ingression, crust failure, and long term two-dimensional MCCI [2]. However, most of the input variables in the models used to date in MCCI analysis, including those characterizing the physical properties of concrete, are not clearly identified in the absence of criteria. In addition, one cannot deny the absence of clarity in the documents and data based on which the physical properties of concrete were derived.

If MCCI analysis is performed using the CORCON-Mod3 model [3,4], it can be verified that the physical properties of concrete, such as its density and melting point, differ with respect to the type of aggregate among the factors governing the characteristics of concrete. However, it is difficult to find a model reflecting the experimental evaluation results of the physical properties of concrete according to the changes in its materials that can be used for a realistic MCCI test and analysis. The current absence of models incorporating the physical properties of concrete mixed with materials produced in Korea should be noted.

This study proposes accurate data gathering and analysis methods for characterizing the physical properties and behavior of concrete at high temperatures seen in severe accidents. To this end, limestone concrete was examined, as well as the mixed composition concrete used in Units 3 and 4 of the ShinKori nuclear power plant.

2. Mix compositions and fabrication of specimens

The properties intended for investigation in this study are mass fraction and melting temperature. To that end, two mix compositions have been considered: one involving siliceous aggregate (the most utilized aggregate in the construction of nuclear power plants) and the other involving limestone aggregate (currently discussed for application to nuclear reactor cavities); the corresponding results have been compared with those of previous research.

2.1. Mix compositions

In order to conduct the experimental evaluation and comparative analysis of the properties of concrete with regard to MCCI, tests were performed on the two mix compositions. These two mix compositions are identical except for the aggregates so as to assess the effect of the gravels and sand on the mass fraction and melting temperature of concrete. In particular, the concrete was fabricated to have identical types and quantities of cement, fly ash, and water. Here, SS indicates the mix with siliceous coarse aggregate and siliceous fine aggregate, and LL indicates the mix with limestone coarse aggregate and limestone fine aggregate.

2.2. Fabrication of specimens

All the specimens are fabricated as ϕ 100 $\times$ 200 mm^2 cylinders to comply with the standard American Society for Testing and Materials (ASTM) C 39. The tests were performed on the specimens after 91 days of curing, according to the standard curing method for nuclear power plant concrete. The concrete density is measured on the ϕ 100 $\times$ 200 mm^2 cylindrical specimens. The composition and melting temperature were evaluated using pulverized samples obtained from the specimens.

2.3. Fabrication of pulverized samples and sampling method

The general standard method for the chemical analysis of concrete (ASTM C 1084) recommends that only the cement paste without aggregates is considered [5]. Apart from ASTM C 1084, there is no specification or standard related to the testing of pulverized concrete samples, including the aggregates, as this approach is rarely adopted. Accordingly, reliability of sampling is enhanced by complying with the International Organization for Standardization (ISO) and Korean Standards (KS) standards for the fabrication and sampling processes of samples.

Sampling and sample preparation are performed using the following procedure in compliance with the international ISO 3082 [6] and Korean KS E 3605 [7] standards: The first sampling process is done after the first pulverization of the ϕ

100 × 200 mm^2 cylindrical specimens, and the pulverized powders are then subjected to a second pulverization step before the second sampling process. The specimens used for the preparation of samples for each mix composition enabled two batches of about 7 kg to be obtained, which were pulverized a second time for the fabrication of the samples.

As this study intended to evaluate the content of H_2O among the mass fractions of concrete, drying that could affect the moisture inside the samples was not executed. In the fabrication process of the samples, the first pulverization step is performed using a jaw crusher and a pestle, and the so-obtained powder is then subjected to a second pulverization step using a ball mill so as to obtain a fine powder. All the samples are subjected to two successive pulverization processes and stirred together so as to obtain uniformly mixed samples. After the second pulverization step, the samples are passed through Sieve No. 100 (graduation of 150 μm) and the particles that have passed through are sampled using cone and quartering.

The reliability is confirmed by research on the establishment of specifications requiring the re-examination and re-execution of the preparation and sampling processes of all the samples in the case where the values of five analysis results per sample exceeds the average by ± 5%.

2.4. Storage and transport of samples

The fabricated samples are stored in sealed glass vial bottles. These vials are transported after sealing them once again in a moisture-free airtight container to prevent the samples from coming in contact with the atmospheric moisture.

3. Concrete density

3.1. Purpose of density measurement

The density and pure mass of concrete were measured to find out the specific gravity and percentage of water absorption. In addition, all the changes in the state of concrete were measured during the concrete density measurement, including the oven-dry mass in which the moisture in concrete was completely dried and the saturated mass after immersion in which concrete was water saturated. This was done in order to compute the density of concrete over all water absorption ranges.

3.2. Measurement method

All the measurements were performed strictly in compliance with the specifications of ASTM C 642-13 [8]. The tests were performed on a series of three specimens per mix composition and each measurement was carried out separately as follows.

3.2.1. Oven-dry mass

The oven-dry mass of specimens is measured that have been dried for more than 24 hours in an oven at 110 ± 5°C at 91 days from placing of specimens. After drying, the specimens are drawn out from the oven and exposed to the air, to cool them down to 20–25°C. After the first measurement of dry mass, the specimens are oven dried once again during 24 hours prior to air drying, and the dry mass is measured once again. Then, oven drying is repeated for 24 hours and measurements are performed for the third time. Verification is done to ensure that the difference between two measurements remains below 0.5%. In case results exceed this range of 0.5%, the previous drying and cooling processes are repeated and the measurement result falling within an error limit of 0.5% is set as the oven-dry mass (designated by A).

3.2.2. Saturated mass after immersion

After the measurement of the oven-dry mass, the surface-dry saturated mass is derived by immersing the specimens in water for > 48 hours at a temperature of ~21 °C. During the measurement, water is removed from the surface using a dry cloth so as to measure the pure mass of the water-saturated specimens.

Similar to the measurement of the oven-dry mass, a measurement is taken once before immersing the specimens in water for more than 24 hours, and the mass is measured a second time. The results are then compared to verify if the error range falls below 0.5%. Where the error exceeds 0.5%, the saturated mass after immersion with an error of < 0.5% is determined using additional measurements (designated by B).

3.2.3. Saturated mass after boiling

Subsequent to the measurement of the saturated mass after immersion, the specimens are immersed in water and the container is heated for 5 hours. Then the specimens are cooled for > 14 hours until their temperature reaches 20–25°C, to measure the mass of the specimens. Here also, as with the measurement of the saturated mass after immersion, water is removed from the surface using a dry cloth and the pure mass of a specimen is measured so as to determine the saturated mass after boiling (designated by C).

3.2.4. Immersed apparent mass

Following the measurement of the saturated mass after immersion and saturated mass after boiling, the immersed apparent mass (designated by D) is determined by directly measuring the mass of the specimen in water using a scale.

3.3. Computation of density

Based on the abovementioned measurement results, the initial bulk density, dry bulk density, and apparent density are computed using Eqs. (1–7). The results are arranged in Section 6.1 per mix composition.

$$\text{Absorption after immersion } (\%) = [(B - A)/A] \times 100 \quad (1)$$

$$\text{Absorption after immersion and boiling } (\%) = [(C - A)/A] \times 100 \quad (2)$$

$$\text{Bulk density, dry} = g_1 = [A/(C - D)] \cdot \rho \quad (3)$$

$$\text{Bulk density after immersion} = [B/(C - D)] \cdot \rho \quad (4)$$

$$\text{Apparent density} = g_2 = [A/(A - D)] \cdot \rho \quad (5)$$

$$\text{Bulk density, initial} = g_3 = [I/(C-D)]\cdot\rho \quad (6)$$

$$\text{Bulk density after immersion and boiling} = g_4 = [C/(C-D)]\cdot\rho \quad (7)$$

where A = oven-dry mass (g); B = saturated mass after immersion (g); C = saturated mass after boiling (g); D = immersed apparent mass (g); g_1 = dry bulk density (kg/m^3); g_2 = apparent bulk density (kg/m^3); g_3 = initial bulk density (kg/m^3); g_4 = bulk density after immersion and boiling (kg/m^3); and ρ = specific gravity of water (1 Mg/m^3 = 1 g/cm^3).

4. Measurement of mass fraction

4.1. Analysis of CO_2 and H_2O by thermogravimetric analysis

Thermogravimetric analysis (TGA) measures the change in the mass of a specimen subjected to heating as a function of time or temperature. In general, TGA is a method for verifying the change in a specific temperature range by maintaining a constant heating rate (increasing the rate of temperature). The sample experiences a loss in its mass within a specific temperature range. This mass loss is mainly provoked by a chemical reaction that generates byproducts in vaporization or phase transition. In particular, the materials are sensitive to the gaseous atmosphere during TGA, which can make the sample react with gases (O_2 and air) when the adopted purge gas is not inert, unlike N_2, He, and Ar. Such reactions can be used to examine decomposition behavior of specimens [9].

The change in the mass is measured continuously using an electronic scale with high sensitivity. The electronic scales used for TGA can be categorized into the horizontal and vertical types. This study used a horizontal-type electronic scale that does not affect the measurement results. Accurate data are acquired by calibrating the interference brought by the buoyancy effect or drag force that can occur during the TGA measurement [10].

In the concrete sector, TGA is mainly used for the analysis of $Ca(OH)_2$, $CaCO_3$, and H_2O. The increase in $CaCO_3$ is primarily examined for the analysis of the degradation of concrete by carbonation or for the analysis of the change in composition caused by the degradation of $Ca(OH)_2$ among the hydrates of concrete [11].

In the present analysis, limestone, as a major component of the aggregate, is composed of CaO (calcium oxide) and is present as a type of calcite in the aggregate in the form of $CaCO_3$. As $CaCO_3$ decomposes into CaO and CO_2 at 550–950°C when heated, TGA is applied for the evaluation of the CO_2 content of the mass fractions.

The TGA equipment is operated to increase the temperature at a rate of 10°C/min from an ambient temperature, and the quantity of sample used during the analysis ranges between 30 mg and 50 mg. This quantity can be modified according to the specifications of the equipment. However, since the analysis is performed using small quantities of sample, it is practically impossible to realize identical quantities. Analysis is therefore conducted with respect to approximate values. In the analysis, the heating temperature is elevated from the ambient temperature to 1,000°C and air is used as a purge gas.

4.2. Analysis of composition by X-ray fluorescence

X-ray fluorescence (XRF) measures the composition of a substance using the white ray (fluorescence) emitted by the X-ray. Since the white ray has the wavelength of the X-ray, the composition of the substance is analyzed using a crystal the lattice constant (d) of which is known after a survey of the white ray in the substance [12].

In summary, when an X-ray is directed on the element present in the sample, the white ray produced secondarily by the X-ray bombardment, which is projected, ejects the electrons covering the element. In order to secure space for the ejected electrons, the orbital electrons move. By measuring the residual energy produced by this motion, it is possible to distinguish the element [10]. Since energy levels differ depending on the element, there is a characteristic value for each element. Accordingly, the released energy can be measure and used to distinguish the element using a crystal with a known lattice constant [13].

In this study, the elements are analyzed in the form of oxides, and the analyzed reference oxides are SiO_2, TiO_2, MnO, MgO, CaO, Na_2O, K_2O, Fe_2O_3, Al_2O_3, Cr_2O_3, and SO_3. For XRF analysis, the whole process running from the fabrication to the analysis of samples could be completed within 3 days by adopting the equipment used for TGA and high-temperature differential thermal analysis (HT-DTA).

As XRF analysis requires solidified samples, samples of 20–30 g are press fabricated in the form of pellets. Here, a binder is mixed with the samples at proportions of 1:1 to 5:1 (binder:sample) to enable pressing. In general, the type of binder adopted for the fabrication of pellets is boric acid. These pellets are analyzed qualitatively in the form of oxides. The analysis speed is set at 20°C/min.

5. Measurement of melting temperature

5.1. High-temperature differential thermal analysis

HT-DTA is a thermoanalytic technique measuring thermal changes, such as reactions, melting, and transitions, occurring during the increase of temperature by heating a sample at a constant rate [11].

Unlike the thermal behavior and heating rate, which remain constant with respect to the elevation of temperature in the chamber, the change in the thermal characteristics is measured according to the change in the state of the sample. The evaluated qualitative thermal change and behavioral difference in a specific temperature change are used in the analysis of the change in the state of the sample [14].

In general, thermal behavior is measured by converting the change in the thermal characteristics of the sample into a voltage that is recorded according to time, where a positive thermal difference defines an upward elevation of temperature and a negative thermal difference defines a downward loss of temperature. The analysis is conducted by comparing the thermal change with respect to a reference substance.

Table 1 – Solidus and liquidus temperatures of various types of concrete (in K and °C) [3].

Concrete type	Temperature (K)		Temperature (°C)	
	Solidus	Liquidus	Solidus	Liquidus
B	1,350	1,650	1,077	1,377
L/S	1,393–1,540	1,568–1,700	1,120–1,267	1,295–1,427
L/L	1,495–1,740	1,875–2,577	1,222–1,467	1,602–2,304
S/S	1,403–1,520	1,523–1,980	1,130–1,247	1,250–1,707
M	1,630	1,920	1,356.85	1,646.85

B, basaltic; L/L, limestone/limestone sand; L/S, limestone/common sand; M, serpentine; S/S, siliceous aggregate/siliceous sand.

Note that since concrete is a compound made of various types of components, it is extremely difficult to derive the characteristics of its standard substances [15]. Therefore, the peaks of the endo- and exothermic reactions are derived experimentally to define the solidus and liquidus temperatures. In this study, the previous literature dedicated to MCCI has been referred to for the melting temperatures of common limestone concrete, limestone common sand concrete, and siliceous concrete.

5.2. *Analysis method*

HT-DTA is performed using a high-temperature thermogravimetric analyzer to examine the melting temperature of concrete, and evaluate the solidus and liquidus temperatures. Air is used as a purge gas during HT-DTA. The heating rate is set at 10°C/min, and the samples are heated up to a temperature of 1,750°C (LL mixes) and 1,650°C (SS mixes). These values were determined after the analysis of the LL mixes for the measurement of the melting temperature based on the measurements carried out up to 1,700°C, which revealed that it becomes impossible to exploit the equipment due to an interaction between the equipment and the sample when heating at temperatures higher than 1,700°C. Table 1 lists the solidus and liquidus temperatures of concrete, with reference to Table 2.2 of CORCON-Mod3 [3], converted into units of Kelvin and Celsius to validate the measured solidus and liquidus temperatures.

6. Analysis results

6.1. *Concrete density*

The oven-dry mass, saturated mass after immersion, saturated mass after boiling, and immersed apparent mass were derived for each mix composition, as shown in Figs. 1 and 2. Moreover, the density of concrete in the state closest to the natural state is also computed by measuring the initial mass. Among these results, particular attention should be given to the initial mass, saturated mass after immersion, and saturated mass after boiling. These three masses are seen to exhibit similar values for each mix composition, which indicates that concrete is completely saturated. In addition, the error for these three types of mass appears to be around 0.1%, which corresponds to a level that can be sufficiently produced by systematic and accidental errors.

Computation of the results complied fully with ASTM C 642. The calculation method of the density described in ASTM C 642 explains that this method does not determine the absolute value of the density. This indicates that the density may change depending on the eventual existence and amount of impermeable pores. However, compared with the general method for computing the density of aggregates, it appears that the density is measured based on identical principles. In this study, the initial density g_3 is used as the measurement executed on concrete in the state closest to that of cast-in-place concrete that has not been subjected to any external environmental change.

For the initial bulk density and bulk density after immersion and boiling obtained for the adopted mix compositions, it is assumed theoretically that all the permeable pores are water saturated. This assumption explains the small difference in the results. In addition, for all the mix compositions, the bulk density after immersion and boiling is smaller than the initial density, which indicates that all the pores are not filled with water in the saturated state after boiling following the oven-dry state.

The average density (initial bulk density) of limestone concrete appeared to be higher than the average density of siliceous concrete by about 4.4%, with a value of 105.5 kg/m^3. As all the materials were applied in identical quantities with the exception of the aggregates, the difference in the density exhibited by limestone concrete could be attributed to its calcite content characterized by a relatively higher specific gravity (Tables 2 and 3).

6.2. *TGA results*

Two different types of equipment are adopted depending on the purpose of the analysis of the mass fraction. TGA equipment is used for the quantitative measurement of the CO_2 and H_2O contents, and XRF equipment is used for the computation of the oxides present in the samples. The following assumptions are adopted for the analysis: (1) in TGA, the physical binding of H_2O evaporates within a temperature range from the ambient temperature to 105°C, and the chemical binding of H_2O decomposes at a temperature between 105°C and 550°C; (2) in TGA, CO_2 decomposes at a temperature between 550°C and 950°C; and (3) in TGA, there is no decomposition of the substances other than H_2O and CO_2 in the temperature range between ambient temperature and 950°C.

The analysis results for each mix composition are described using the analysis results of five samples per mix

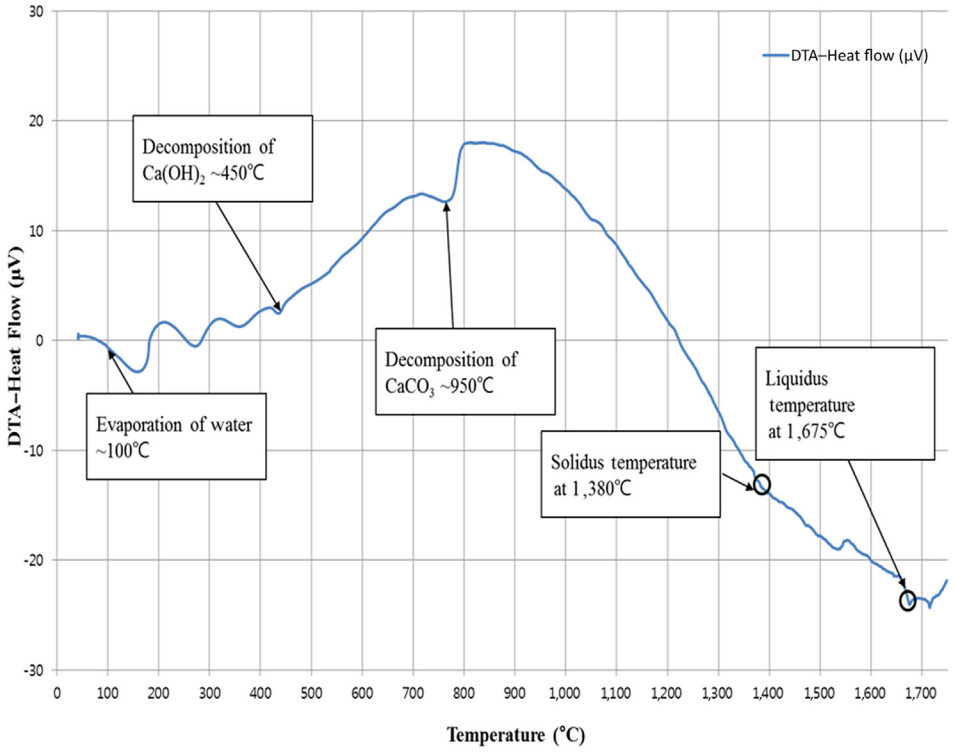

Fig. 1 – Analysis of melting temperature data of LL mixes. DTA, differential thermal analysis; LL, the mix with limestone coarse aggregate and limestone fine aggregate.

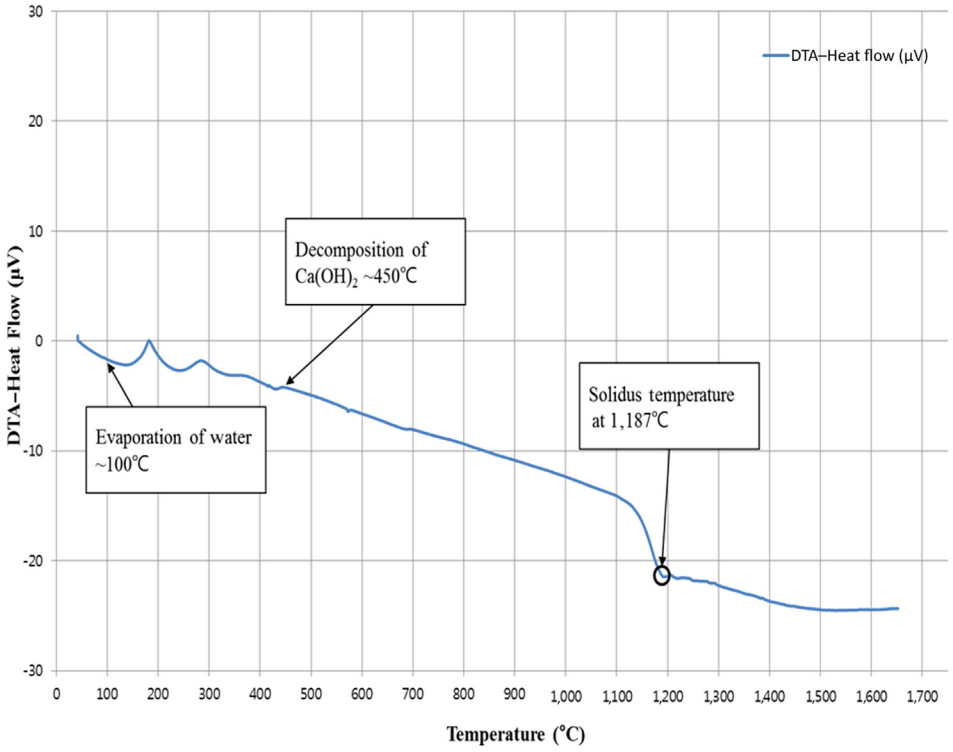

Fig. 2 – Analysis of melting temperature data of SS mixes. DTA, differential thermal analysis; SS, the mix with siliceous coarse aggregate and siliceous fine aggregate.

Table 2 – Density of LL concrete (in kg/m^3).

	LL-1	LL-2	LL-3	Average
Dry bulk density (g_1)	2,264.95	2,261.63	2,268.41	2,265.00
Apparent bulk density (g_2)	2,581.54	2,591.55	2,585.53	2,586.21
Initial bulk density(g_3)	2,391.42	2,394.13	2,388.48	2,391.34
Bulk density after immersion and boiling (g_4)	2,387.58	2,388.93	2,391.07	2,389.19

LL, the mix with limestone coarse aggregate and limestone fine aggregate.

composition and the averages of five samples. The reliability of the analysis results is strengthened by arranging separately the maximum, average, and minimum values for each component. All the results are arranged by mix composition.

In view of the CO_2 analysis results among the major indicators of mass fraction, the LL mixes show the highest results. This can be attributed to the high content of limestone in CaO, leading to a higher CO_2 content for the LL mixes than for the SS mixes.

The results calculated by TGA are expressed in terms of the CO_2 and H_2O contents in Tables 4 and 5 by means of their average, maximum, and minimum values, so as to grasp the error range. It can be seen that the error with reference to the average remains below ± 1% in most cases. For the LL mixes also, the error in the results being less than 3%, there is no need to re-execute the sampling and analysis processes.

6.3. *XRF analysis results*

The results for each mix composition are described using the analysis results of five samples per mix composition and the averages of five samples, and are arranged in Tables 6 and 7. Here, it is assumed that only the measured elements are present. The entire components of concrete being supposed as 98.6% totally in the sum of results in TGA and XRF, which is considered chemical compounds of concrete excluded natural constituent.

In view of the CO_2 analysis results among the major indicators of the mass fraction, the LL mixes show the highest results. This can be attributed to the high content of limestone in CaO, which produces higher CO_2 for the LL mixes than for the SS mixes.

Moreover, as explained above for the analysis of TGA results, the high reliability of the analysis results can be verified since the XRF analysis results of each component present an error smaller than ± 0.2% with reference to the averages.

Table 3 – Density of SS concrete (in kg/m^3).

	SS-1	SS-2	SS-3	Average
Dry bulk density (g_1)	2,122.12	2,129.02	2,122.44	2,124.52
Apparent bulk density (g_2)	2,534.33	2,524.95	2,528.63	2,529.30
Initial bulk density(g_3)	2,293.67	2,297.30	2,266.63	2,285.87
Bulk density after immersion and boiling (g_4)	2,284.77	2,285.82	2,283.08	2,284.56

SS, the mix with siliceous coarse aggregate and siliceous fine aggregate.

Table 4 – TGA results of LL concrete mixes (in %).

Sample no.	CO_2	H_2O chemical	H_2O physical	TG total
1	25.90	9.32	0.58	35.80
2	25.95	10.59	0.48	37.02
3	24.54	10.03	0.57	35.14
4	27.69	6.64	0.53	34.86
5	22.98	9.96	0.86	33.80
Average	25.41	9.31	0.60	35.32

LL, the mix with limestone coarse aggregate and limestone fine aggregate; TG, thermogravimetry; TGA, thermogravimetric analysis.

There is, thus, no need to re-execute the sampling and analysis processes.

Table 8 presents the mass fraction. In view of the analysis results of the LL mixes, the amount of CO_2 is similar to that of limestone and common sand of the NUREG report when referring to the chemical analysis results of concrete. However, in view of the amounts of CaO and SiO_2, the results are very close to those of limestone concrete. Accordingly, it can be stated that, among the materials applied in the mix composition of concrete in this study, the characteristics of the aggregates are particularly decisive in the development of the properties of concrete.

6.4. *Melting temperature*

The LL mix is heated up to a maximum temperature of 1,750°C for the analysis. In view of the first analysis results, the solidus and liquidus temperatures appear to be 1,380°C and 1,675°C, respectively. From the second analysis results, these temperatures are 1,380°C and 1,665°C, respectively. The analysis results are plotted in Fig. 1. The analyzed solidus and liquidus temperatures are seen to be, respectively, 1,380°C and 1,670°C, showing a tendency similar to the limestone concrete of CORCON-Mod3.

Fig. 2 plots the analysis results for the SS mixes. It can be seen that the solidus and liquidus temperatures were 1,187°C and 1,385°C, respectively. These results agree with those of Table 1 for siliceous concrete (S/S), which can be attributed to the similarity of the LL mix to the composition of siliceous concrete. However, it is not shown that any kind of singularity around 550°C in the DTA curve in Fig. 2, and it is supposed that the silica type is basaltic (glass) and not quartz (crystal).

Table 5 – TGA results of SS concrete mixes (in %).

Sample No.	CO_2	H_2O chemical	H_2O physical	TG total
1	1.42	5.61	0.84	7.87
2	1.03	5.12	0.60	6.75
3	1.22	5.37	0.46	7.05
4	1.17	5.04	0.35	6.56
5	1.06	5.62	0.74	7.42
Average	1.18	5.35	0.60	7.13

No., number; SS, the mix with siliceous coarse aggregate and siliceous fine aggregate; TG, thermogravimetry; TGA, thermogravimetric analysis.

Table 6 – Composition of LL concrete mixes by XRF analysis (in %).

Formula	Sample No. 1	Sample No. 2	Sample No. 3	Sample No. 4	Sample No. 5	Average
SiO_2	11.54	11.47	11.33	11.32	11.34	11.40
TiO_2	0.24	0.26	0.25	0.26	0.24	0.25
MnO	0.06	0.06	0.07	0.06	0.07	0.07
MgO	2.02	2.02	1.99	1.97	1.95	1.99
CaO	77.05	77.13	77.34	77.41	77.37	77.26
Na_2O	0.53	0.53	0.52	0.50	0.50	0.52
K_2O	1.26	1.26	1.26	1.27	1.24	1.26
Fe_2O_3	2.73	2.75	2.73	2.74	2.76	2.74
Al_2O_3	3.24	3.20	3.19	3.14	3.20	3.19
Cr_2O_3	0.01	0.01	0.01	0.01	0.01	0.01

LL, the mix with limestone coarse aggregate and limestone fine aggregate; No., number; XRF, X-ray fluorescence.

Table 7 – Composition of SS concrete mixes by XRF analysis (in %).

Formula	Sample No. 1	Sample No. 2	Sample No. 3	Sample No. 4	Sample No. 5	Average
SiO_2	58.05	58.16	58.07	58.33	58.02	58.13
TiO_2	0.49	0.50	0.50	0.49	0.49	0.50
MnO	0.08	0.09	0.08	0.08	0.08	0.08
MgO	2.11	2.18	2.13	2.16	2.19	2.15
CaO	19.21	19.13	19.17	18.93	18.99	19.09
Na_2O	1.56	1.58	1.65	1.63	1.66	1.62
K_2O	3.24	3.21	3.22	3.23	3.23	3.23
Fe_2O_3	3.66	3.61	3.62	3.56	3.61	3.61
Al_2O_3	10.12	10.09	10.12	10.14	10.22	10.14
Cr_2O_3	0.02	0.02	0.02	0.03	0.02	0.03

No., number; SS, the mix with siliceous coarse aggregate and siliceous fine aggregate; XRF, X-ray fluorescence.

Table 9 lists the melting temperatures derived from the analysis. A literature survey for the comparison of the analysis results with previous research results revealed the difficulty of such a task due to the lack of studies focusing on the characteristics of concrete. Most of the studies dealing with the properties of concrete used limestone coarse aggregate/common sand, rendering it more difficult to validate the results of this study, which applies limestone and siliceous aggregate identically as coarse aggregate/fine aggregate. In the case of analytic research, most of the properties of concrete reflected in the analysis are not even referred to a source. Accordingly, a comparison is performed based on the mass fraction and melting temperature presented in the NUREG report [3].

7. Conclusion

This study conducted an analysis of the mass fraction and melting temperature, and the measurement of the density of concrete to evaluate the MCCI appropriateness of limestone concrete.

Despite the slight difference, as compared with previous research, in the characteristic values of concrete the results of this research remain within the boundaries defined by the maximum and minimum values reported in previous studies. This indicates that the results derived in this study exhibit high reliability. The following summarizes the conclusions of this study. (1) This study examined experimentally the density, mass fraction, and melting temperature of siliceous concrete and limestone concrete. The results were seen to be highly reliable in view of the small errors achieved owing to the repeated measurements conducted in the tests. (2) The density of limestone concrete appeared to be ~4.5% higher due to the high content in $CaCO_3$ calcite in the composition of the aggregates. (3) Mass fractions similar to those of previous

Table 8 – Representative concrete mass fraction data of NUREG report [3] and analysis results of LL and SS concrete mixes.

Formation	NUREG report (%) (CORCON data)			Results (%) (this study)	
	S/S	L/S	L/L	LL	SS
SiO_2	69.00	35.80	3.60	7.37	54.01
TiO_2	0.80	0.18	0.12	0.16	0.46
MnO	0.00	0.03	0.01	0.04	0.08
MgO	0.70	0.48	5.67	1.29	2.00
CaO	13.50	31.30	45.40	49.97	17.73
Na_2O	0.70	0.08	0.01	0.33	1.50
K_2O	1.40	1.22	0.68	0.81	3.00
Fe_2O_3	1.00	1.44	1.20	1.77	3.36
Al_2O_3	4.00	3.60	1.60	2.06	9.42
Cr_2O_3	0.00	0.01	0.00	0.01	0.02
CO_2	4.23	21.15	35.70	25.41	1.18
H_2O chemical	3.10	2.70	3.94	9.31	5.35
H_2O physical	3.68	2.00	2.00	0.60	0.60

L/L, limestone/limestone sand; LL, the mix with limestone coarse aggregate and limestone fine aggregate; L/S, limestone/common sand; SS, the mix with siliceous coarse aggregate and siliceous fine aggregate.

Table 9 – Representative concrete melting temperature of NUREG report [3] and analysis results of LL and SS concrete mixes.

	Melting temperature (°C)				Notes
	L/L	LL	S/S	SS	
Liquidus	1,222–1,467	1,380	1,602–2,034	1,670	CORCON-Mod3 Table 2.2 (L/L, S/S)
Solidus	1,130–1,247	1,187	1,250–1,707	1,385	Measured using HT-DTA equipment (LL, SS)

HT-DTA, high-temperature differential thermal analysis; L/L, limestone/limestone sand; LL, the mix with limestone coarse aggregate and limestone fine aggregate; L/S, limestone/common sand; SS, the mix with siliceous coarse aggregate and siliceous fine aggregate.

research results were derived for both types of concrete. A comparison of the two most important components revealed that the mass fraction of CaO in SS concrete was higher than that in LL concrete by ~31%, but was lower by 65.4% in the case of SiO_2. (4) The derived melting temperature was also found to be within the ranges reported in previous studies. Compared with the LL mixes, the solidus and liquidus temperatures of the SS mixes were higher by 198°C and 290°C, respectively.

The characteristics developed by concrete are subordinate to the type and amount of the binder, the quantity of water, and the type of aggregate adopted in the mix. In general, the mix proportions are set to approximately 13 (binder):7 (water):73 (aggregates, including fine and coarse aggregates). The mass fraction and melting temperature of concrete depend on the quantity of its components. Therefore, before the analysis, it is imperative to examine the effect of the aggregate as being the material occupying the largest proportion in the mix. Since this study undertook the experimental evaluation of concrete only, additional studies should be conducted to investigate the MCCI between concrete and the characteristics of each type of aggregate.

Acknowledgments

This work was supported by the Nuclear Power R&D Program of the Korea Institute of Energy Technology Evaluation and Planning (KETEP) grant funded by the Korea government Ministry of Knowledge Economy (No. 2011T100200161).

REFERENCES

[1] M.T. Farmer, B.W. Spencer, B.R. Seghal, MACE Core Coolability Test M1B, 20th Water Reactor Safety Meeting, Bethesda, MD, 1992.

[2] R.E. Blose, J.E. Gronager, A.J. Suo-Anttila, J.E. Brockmann, SWISS: sustained heated metallic melt/concrete interactions with overlying water pools, NUREG/CR4727, SANDS85-1546 R#, R4, R7, 1987.

[3] CORCON-MOD3: An Assessment of the CORCON-MOD3 Code Part I: Thermal-Hydraulic Calculations, International Agreement Report, NUREG/IA-0129 Part I, U.S. Nuclear Regulatory Commission.

[4] CORCON-MOD3: An Integrated Computer Model for Analysis of Molten Core–Concrete Interactions User's Manual, NUREG/CR-5843 SAND92–0167, U.S. Nuclear Regulatory Commission.

[5] ASTM C 1084. Standard Test Method for Portland-Cement Content of Hardened Hydraulic-Cement Concrete.

[6] ISO 3082. Iron Ores—Sampling and Sample Preparation Procedures.

[7] KS E 3605. Particulate Materials—General Rules for Methods of Sampling.

[8] ASTM C 642. Standard Test Method for Density, Absorption, and Voids in Hardened Concrete.

[9] KS M ISO 11358. Plastics—Thermogravimetry (TG) of Polymers—General principles.

[10] H.J. Lee, J.H. Lee, M.S. Cho, D.G. Kim, Analysis of Carbonation Properties of NPP Concrete Using Thermogravimetric and X-ray Diffraction Method, Vol. 24, No. 1, Korea Institute of Concrete, 2012.

[11] S.G. Park, Principal and usage of TG-DTA, Cement 65 (1976) 25–31.

[12] S.H. Park, A Comparative Study on Analyzing Methods for Improving the Efficiency of the Heavy Metal Exposure Assessment, Occupational Safety and Health Research Institute, 2000.

[13] KS E ISO 9516–1. Iron Ores—Determination of Various Elements by X-Ray Fluorescence Spectrometry—Part 1: Comprehensive procedure.

[14] KS D 0069. Method of Determining the Crystallization Temperatures of Amorphous Metals.

[15] KS M ISO 11357–3. Plastics—Differential Scanning Calorimetry (DSC)—Part 3.